Aerodynamic Performance Analysis of Penguin-Inspired Biomimetic Aircraft Wing

Mahadi Hasan Masud and Peter Dabnichki

Nomenclature

Re	Reynolds number
AOA	Angle of attack
CD	Coefficient of drag
CL	Coefficient of lift
RANS	Reynolds-averaged Navier–Stokes
NURBS	Non-uniform rational basis spline
CFL	Courant–Friedrichs–Lewy

1   Introduction

Improved aerodynamic efficiency through reduction in the drag force complemented by increased lift force has been the objective of the aerospace industry. Traditional large-scale aircrafts have had their wing profiles substantially altered in the last decade and the lift to drag ratio considerably reduced while operating at low Reynolds number (Re). Moreover, the introduction of micro aerial vehicles posed further challenges as they run at low Re, where stall occurs at a very low AOA. A substantial volume of research explores an increased aerodynamic efficiency for a wide range of AOA and Re using modified aerofoil's shape and surface. In search of such solutions, sinusoidal leading edge and dimpled surface have been introduced, inspired by biomimetic research. One of the most significant biomimetics aerodynamic applications in recent years is the modified aerofoil inspired by the humpback

M. H. Masud (✉) · P. Dabnichki
School of Engineering, RMIT University, Bundoora Campus, Melbourne, Australia
e-mail: masud.08@me.ruet.ac.bd; peter.dabnichki@rmit.edu.au

whale flipper structure. The bumps along the leading edge of the humpback whale flippers are arranged sinusoidally as rounded tubercles. Protuberances along the leading edge, known as LEP, help the flipper hydrodynamically by functioning as a passive flow controller (Watts & Fish, 2001). Malipeddi et al. analyzed modified NACA2412 foil with a sinusoidal leading edge and found that the maximum lift coefficient can be increased by up to 48% at an angle of attack of 16 deg when compared to baseline aerofoil (Malipeddi et al., 2012). Miklosovic et al. examined modified NACA0020 wing at a Re= 5.2×10^5 and found that the lift coefficient increases by 60%, while the drag coefficient decreased by 32% (Miklosovic et al., 2004). Furthermore, extensive research on surface modification is ongoing by introducing vortex generators that help to reduce the pressure drag at a high AOA and bring overall performance improvement (Huang & Lin, 1995; Bearman & Owen, 1998; Akbari & Price, 2003).

There is, however, a much broader scope for research on underwater "flying" features that could potentially deliver improved aerodynamic performance, in particular for small-scale aircrafts that require agility and high-energy efficiency due to their limited energy supply. Based on kinematic data analysis of numerous penguin dives, Masud et al. showed that penguin species offer efficient underwater propulsion (Masud et al., 2022). Hence, we hypothesize that their blade-shaped wings would offer a higher stall angle. However, to date, no study investigated the drag and lift characteristics of a penguin-inspired biomimetic wing under different flow conditions. In this work, computational fluid dynamics analysis of aerodynamic forces of a penguin-inspired wing is performed to assess its suitability for aircraft application with a focus on AOA and stall.

2   Penguin-Inspired Wing Model and Numerical Procedure

The wing model was devised from a scan of a dead little (aka fairy penguin) penguin. The carcass was provided from the Philp Island research group (Permit no.: 10009208 under Wildlife Act 1975) and scanning of the little penguin carcass was performed using a HandySCANTM® 3D (Volumetric accuracy: 0.020 mm + 0.100 mm/m) scanner. The 3D scan of a little penguin carcass was transformed into a NURBS solid. For converting the STL (mesh) files into non-uniform rational basis spline (NURBS) SOLID, Autodesk Meshmixer® and GEOMAGIC DESIGNX® 2016 software were used. Then we scaled the dimension two times that make the wingspan 0.24 m, and correspondingly, the chord length across the span also changed. After converting the STL (mesh) into NURBS, we took a cross-section from the mid-plane (spanwise) of the wing having a chord length of 0.108 m and extruded it up to the length of 0.108 m. That means the generated penguin-inspired wing has a chord*span of ($C = 0.108$ m * $S = 0.108$ m), as shown in Fig. 1 at an AOA = 10 deg.

The computer-aided design model was transferred to ANSYS Fluent® 2021, and the computational domain's dimensions were set to 30C*20C*10C
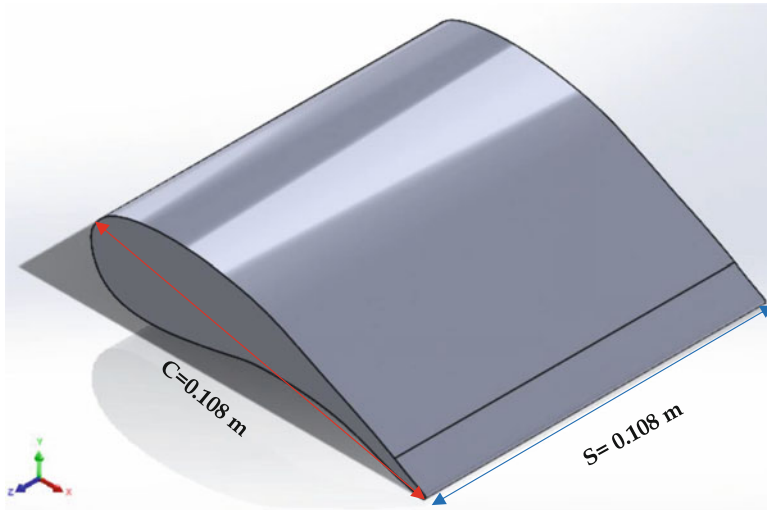
Fig. 1 Penguin-inspired biomimetic wing

(length*height*depth). The boundary's inflow and outflow are 10C upstream and 20C downstream from the wing's leading edge and trailing edge, respectively. In relation to the height, it is placed precisely in the middle of the computational domain. The simulation was performed at a chord-based Re $= 5 \times 10^5$ related to air velocity for $V_{avg} = 67.7$ m/s at an angle of attack ranging from 0 to 30 deg. In order to compare the results with the available experimental data of the conventional baseline NACA0012 wing (Critzos et al., 1955) at the same Reynolds number, Re $= 5 \times 10^5$ was selected. Furthermore, Kowalczuk et al. stated that Courant–Friedrichs–Lewy (CFL) also known as Courant with a value of 1 is adequate for sufficiently accurate results (Kowalczuk & Tatara, 2021). Hence, CFL of 1 was used, and for that, the time step was fixed at 10^{-3} s. Each solution was conducted for a minimum duration of 2 s, and the initial 100 steps were eliminated to mitigate the effect of initial flow conditions.

In meshing, 15 inflation layers were defined with a growth ratio of 1.2 to accurately resolve the boundary layer. Delayed detached Eddy simulation along with improved delayed detached Eddy simulation as shielding function was used, where SST K-ω model was applied as RANS model. Thus, to determine the turbulence near the wall, we needed to obtain the average Y+ value ≤1, and to obtain desired Y+ value, the first layer thickness of the inflation layer was set at 4.8×10^{-6} for an air velocity of 67.7 m/s. The maximum skewness and orthogonal quality of the generated mesh were 0.83 and 0.998, respectively. Finally, the mesh sensitivity analysis was performed following the procedure mentioned in Elsayed and Lacor (2011).

3   Results and Discussion

The lift coefficient (C_L) of the baseline aerofoil shows linear relationship up to about 10 deg AOA and has a better drag to lift ratio when compared with the findings of Critzos et al. (1955). The penguin-inspired profiles are also streamlined bodies and flow separation occurs beyond 20 deg AOA at a Re = 5×10^5, after which point, C_L begins to decrease with further rise of the AOA. In other words, nearly 100% increase in the flow separation threshold is achieved compared to the NACA0012 threshold value. Hence, there is a strong suggestion that penguin-inspired biomimetic aerofoil promises better performance compared to almost all aerofoils in relation to stall effect (Airfoil Tools, 2022). It is already stated in the literature that protuberances along the leading edge of the aerofoil display better performance compared to the baseline aerofoils, specifically at higher AOA; this improved performance is owing to a notable reduction/delay of the flow separation (Levshin et al., 2006; Johari et al., 2007; Cai et al., 2019; Wang et al., 2021). This additional modification on a modified NACA aerofoil delivers inferior performance compared to the penguin-inspired biomimetic aircraft wings in terms of regulating flow separation at higher AOA.

The drag coefficient is proportional to the AOA for streamlined bodies (Masud et al., 2017; Islam et al., 2018), which is also the case in this work (see Fig. 2 for details). For AOA of 30 deg, a maximum drag coefficient of 0.35 is reached, which is still 71.4% lower than the baseline aerofoil of 0.60 (Critzos et al., 1955). Hence, it can be concluded that the penguin-inspired biomimetic aircraft wings offer superior performance compared to the baseline aerofoil beyond 10 deg AOA. Furthermore, the lift-to-drag ratio for penguin-inspired biomimetic aircraft wings is maximum when AOA is at 10 deg, and it is anticipated that the efficiency will also be the highest at that point. The combination of those results points to overall better maneuverability at lower energy cost.

4   Conclusion

We have numerically evaluated the aerodynamic performance of the penguin-inspired biomimetic aircraft wing, compared the results with the experimental data of baseline NACA0012 aerofoil for Re = 5×10^5, and found that the stall occurs for NACA0012 at around 10 deg AOA. It is notable that for a penguin-inspired biomimetic aircraft wing, stall occurs at 20 deg (at the same Reynolds number). Moreover, in the post-stall region, the penguin-inspired biomimetic aircraft wing provides superior results compared to baseline NACA0012 aerofoil. At 15 deg and 20 deg AOA, penguin-inspired biomimetic aircraft wings provide 30.43% and 52.11% greater lift compared to the reported lift for NACA0012 aerofoil, respectively. Moreover, under the same conditions, penguin-inspired biomimetic aircraft wings generate 6.25% and 9.1% lesser drag compared to the reported drag for
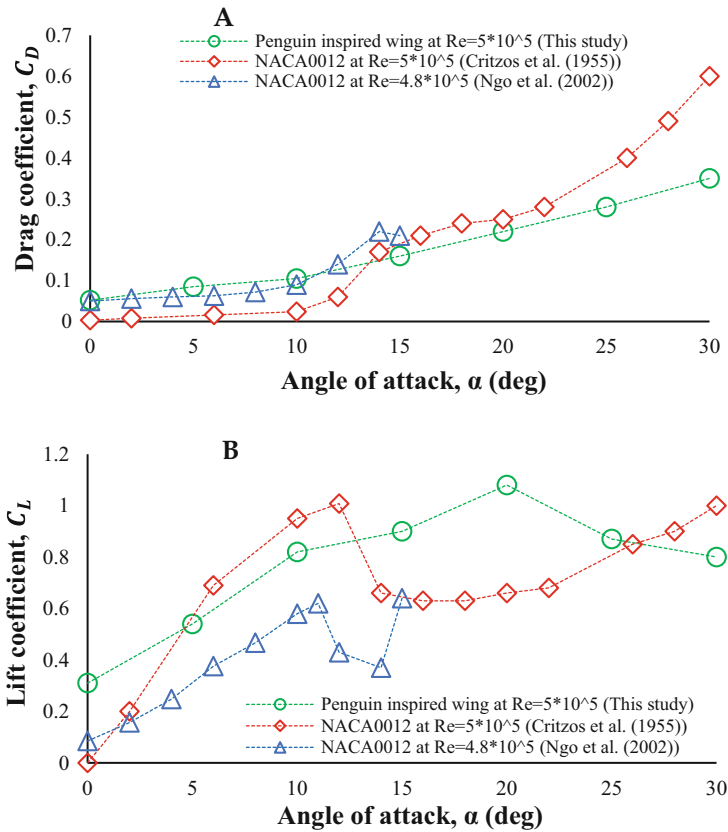
Fig. 2 Aerodynamic forces of a penguin-inspired biomimetic aircraft wing at different AOA. (**a**) Variation in drag coefficient with varying AOA, (**b**) variation in lift coefficient with varying AOA

NACA0012 aerofoil, respectively. Finally, it can be concluded that although penguin-inspired biomimetic aircraft wings show potential to be implemented as biomimetic aircraft wings for high maneuverability aircraft with potentially reduced energy requirements due to the demonstrated drag reduction, these are initial results, and further numerical and experimental analysis at varying flow conditions is required to fully assess their suitability for practical applications.

References

Airfoil Tools. (2022). *NACA 4 digit Airfoil database*. Available at http://airfoiltools.com/search/index?m%5Bgrp%5D=naca4d&m%5Bsort%5D=1. Accessed 4 Apr 2022.

Akbari, M. H., & Price, S. J. (2003). Simulation of dynamic stall for a NACA 0012 airfoil using a vortex method. *Journal of Fluids and Structures*. Elsevier, *17*(6), 855–874.

Bearman, P. W., & Owen, J. C. (1998). Reduction of bluff-body drag and suppression of vortex shedding by the introduction of wavy separation lines. *Journal of Fluids and Structures*. Elsevier, *12*(1), 123–130.

Cai, C., Liu, S., Zuo, Z., Maeda, T., Kamada, Y., Li, Q. A., & Sato, R. (2019). Experimental and theoretical investigations on the effect of a single leading-edge protuberance on airfoil performance. *Physics of Fluids*. AIP Publishing LLC, *31*(2), 27103.

Critzos, C. C., Heyson, H. H., & Boswinkle, R. W., Jr. (1955). *Aerodynamic characteristics of NACA 0012 airfoil section at angles of attack from 0 deg to 180 deg*. National Aeronautics and Space Administration.

Elsayed, K., & Lacor, C. (2011). Numerical modeling of the flow field and performance in cyclones of different cone-tip diameters. *Computers & Fluids*. Elsevier, *51*(1), 48–59.

Huang, R. F., & Lin, C. L. (1995). Vortex shedding and shear-layer instability of wing at low-Reynolds numbers. *AIAA Journal, 33*(8), 1398–1403.

Islam, M. T., Arefin, A. M., Masud, M. H., & Mourshed, M. (2018). The effect of Reynolds number on the performance of a modified NACA 2412 airfoil. In *AIP conference proceedings*. https://doi.org/10.1063/1.5044325

Johari, H., Henoch, C., Custodio, D., & Levshin, A. (2007). Effects of leading-edge protuberances on airfoil performance. *AIAA Journal, 45*(11), 2634–2642.

Kowalczuk, Z., & Tatara, M. S. (2021). Analytical 'steady-state'-based derivation and clarification of the Courant-Friedrichs-Lewy condition for pipe flow. *Journal of Natural Gas Science and Engineering*. Elsevier, *91*, 103953.

Levshin, A., Custodio, D., Henoch, C., & Johari, H. (2006). Effects of leading edge protuberances on airfoil performance. In *36th AIAA fluid dynamics conference and exhibit* (p. 2868).

Malipeddi, A., Mahmoudnejad, N., & Hoffmann, K. (2012). Numerical analysis of effects of leading-edge protuberances on aircraft wing performance. *Journal of Aircraft, 49*(5), 1336–1344.

Masud, M. H., Naim-Ul-Hasan, Arefin, A. M. E., & Joardder, M. U. (2017). Design modification of airfoil by integrating sinusoidal leading edge and dimpled surface. In *AIP conference proceedings*. https://doi.org/10.1063/1.4984677

Masud, M. H., La Mantia, M., & Dabnichki, P. (2022). Estimate of Strouhal and Reynolds numbers for swimming penguins. *Journal of Avian Biology*. Wiley Online Library, *2022*(2), e02886.

Miklosovic, D. S., Murray, M. M., Howle, L. E., & Fish, F. E. (2004). Leading-edge tubercles delay stall on humpback whale (Megaptera novaeangliae) flippers. *Physics of Fluids, 16*(5), 39–42. https://doi.org/10.1063/1.1688341

Wang, T., Feng, L.-H., & Li, Z.-Y. (2021). Effect of leading-edge protuberances on unsteady airfoil performance at low Reynolds number. *Experiments in Fluids*. Springer, *62*(10), 1–13.

Watts, P., & Fish, F. (2001). The influence of passive, leading edge tubercles on wing performance. In *Proceedings of the twelfth international symposium on unmanned untethered submersible technology (UUST)*. Autonomous Undersea Systems Institute.